JOURNAL OF EXPERIMENTAL AND THEORETICAL PHYSICS, 2025, Vol. 167, No. 1, pp. 124–135

STATISTICAL, NONLINEAR, AND SOFT MATTER PHYSICS

SUPRATHERMAL ELECTRON TRANSPORT IN WEAKLY AND STRONGLY MAGNETIZED ASTROPHYSICAL PLASMAS INCLUDING COULOMB COLLISIONAL EFFECTS

© 2025 Ji-Hoon Ha

Korea Space Weather Center, Korea AeroSpace Administration, Jeju, South Korea
e-mail: hjhspace223@gmail.com

Received July 01, 2024

Revised August 15, 2024

Accepted August 20, 2024

Abstract. This study examines electron transport in astrophysical plasmas mediated by Coulomb collisions and collisionless wave-particle interactions, using a kinetic transport model that incorporates spectral evolutions through these interactions. It investigates the transport of suprathermal electrons via whistler turbulence and the effects of plasma magnetization. Key findings indicate that in strongly magnetized plasmas, diffusion timescales in pitch angle space become saturated at large pitch angles, independent of increasing magnetic field strength. Conversely, in weakly magnetized plasmas, these timescales decrease with decreasing magnetic field strength, enhancing electron transport in velocity space. The study also identifies minimum conditions for resonant scattering, dominated by wave-particle interactions over Coulomb collisions, which depend on Coulomb collision effects and the power-law slope of the whistler turbulence spectrum. These findings have applications in weakly magnetized astrophysical plasmas, from the relatively strong magnetic fields of the interplanetary medium to the very weak magnetic fields of the intracluster medium.

DOI: 10.31857/S0044451025011le6

1. INTRODUCTION

Plasma physics is essential for understanding various astrophysical and laboratory phenomena, where electron transport significantly influences the behavior and evolution of plasma systems. In the field of fusion plasma, plasma heating and current drive have been primarily examined to maintain the conditions necessary for the magnetic confinement of plasmas [1]. It has been demonstrated that the propagation and damping of radiofrequency waves, including ion cyclotron, electron cyclotron, and lower-hybrid waves, produce energetic ions and electrons through Landau and cyclotron damping, which leads to current drive generation in the plasma system. Along with such collisionless damping, the collisional relaxation of energetic particles is involved in the evolution of particle distribution in the plasma system. Likewise, collisionless wave-particle interactions and collisional relaxation also play a crucial role in particle transport in astrophysical plasmas. Indeed, turbulence and the associated plasma instabilities are ubiquitous in astrophysical plasmas, and understanding energy transport through such turbulence is a long-standing problem [2–5].

Plasma phenomena and their dynamical evolution in space and astrophysical plasmas depend on the magnetization, defined as follows:

$$\frac{\omega_{pe}}{\Omega_e} = \frac{\sqrt{4\pi n_0 e^2 / m_e}}{eB_0 / m_e c} \propto \frac{\sqrt{n_0}}{B_0}, \qquad (1)$$

where

$$\omega_{pe} = \sqrt{4\pi n_0 e^2 / m_e}, \quad \Omega_e = eB_0 / m_e c$$

stand for the plasma frequency and electron gyrofrequency, respectively, and these quantities depend on the plasma density n_0 and magnetic field B_0. Thus, the phenomena associated with plasma physics have been examined across a wide range of magnetization factors [6–11]. For instance, the characteristics of plasma instabilities in space plasma depend on the properties of the medium, such as strongly magnetized plasma in the solar atmosphere near the Sun ($\omega_{pe} / \Omega_e < 1$) and weakly magnetized plasmas in the solar wind propagating

toward Earth ($\omega_{pe}/\Omega_e > 1$) [6, 7]. Additionally, a wide range of ω_{pe}/Ω_e can be adopted to model the pulsar wind propagation from the strongly magnetized magnetosphere of a pulsar to the weakly magnetized pulsar wind nebulae propagating toward the interstellar medium [8, 9]. Furthermore, rigorous theories have been proposed for kinetic turbulence and their roles in particle heating through energy transfer in ambient astrophysical environments, including weakly magnetized media such as interplanetary, interstellar, and intracluster media ($\omega_{pe}/\Omega_e \gg 1$) [10, 11].

Understanding turbulence and dynamical evolution in various astrophysical media is crucial for comprehending particle transport across strongly magnetized to weakly magnetized plasmas, which is essential to examine the nature of plasma distribution in various space and astrophysical plasmas. The mechanisms behind particle transport in space weather have been particularly examined so far. Indeed, suprathermal electrons have been observed by the Parker Solar Probe in the interplanetary medium; these electrons are expected to originate in the solar corona and escape into the interplanetary medium along open magnetic field lines [12, 13]. While particle transport in plasmas has primarily been attributed to Coulomb collisions, observational evidence of suprathermal electrons highlights the importance of collisionless wave-particle interactions. In this regard, recent theoretical studies have proposed a kinetic model based on the Fokker-Planck equation, including wave-particle interactions mediated by plasma turbulence [14–23]. For instance, Kim et al. [14] highlighted that the persistence of a non-Maxwellian distribution in the solar wind could be exhibited through wave-particle interactions due to Langmuir turbulence in the absence of Coulomb collisions (see also [15]). Tang et al. [16] incorporated Coulomb collisional effects along with wave-particle interaction terms into the kinetic model and showed that Coulomb collisions predominantly transport core electrons following a Maxwellian distribution, whereas suprathermal electrons are preferentially accelerated through whistler turbulence. Simulation studies using the particle-in-cell (PIC) method have also shown the formation of suprathermal electrons through whistler turbulence [24, 25]. These findings are consistent with observational evidence of suprathermal electrons in interplanetary space [12, 13].

Despite the considerable progress mentioned above, several gaps persist in our understanding, particularly regarding how these mechanisms operate under different plasma magnetization conditions. Notably, the plasma parameters, including magnetization, differ between interplanetary space and other astrophysical media such as interstellar and intracluster media. Consequently, plasma phenomena related to particle transport could also differ. While simulation studies using kinetic plasma simulations have demonstrated possible acceleration mechanisms through collisionless shocks and turbulence in various astrophysical media [26–31], it is essential to understand the transport of such accelerated particles in these media to demonstrate the persistence of non-Maxwellian distributions.

In this context, this work aims to improve our understanding of particle transport theory based on the kinetic transport equation and whistler turbulence under different plasma magnetization conditions relevant to various astrophysical media. To achieve this, we adopt a kinetic transport model that incorporates the spectral evolution influenced by both Coulomb collisions and wave-particle interactions, as proposed in previous works [16–19]. By examining how suprathermal electrons are transported through whistler turbulence under varying degrees of plasma magnetization, we extend the applicability of the kinetic transport model to various astrophysical environments. This work reveals distinct behaviors in diffusion timescales for weakly and strongly magnetized plasmas, with significant implications for electron transport dynamics. Additionally, we identify minimum conditions for resonant scattering dominated by wave-particle interactions over Coulomb collisions, highlighting dependencies on Coulomb collision effects and the power-law slope of the whistler turbulence spectrum. This comprehensive approach allows us to explore diffusion timescales in both velocity and pitch angle space, providing new insights into the underlying processes governing electron transport in plasmas.

2. DESCRIPTION OF THE KINETIC MODEL

The evolution of the electron velocity distribution function in astrophysical environments has been examined using the kinetic transport equation [16–19]. The electromagnetic interaction in a typical astrophysical environment includes the electric force and the Lorentz force, which are described as follows:

$$\mathbf{a} = -\frac{e\mathbf{E}}{m_e} - \frac{e}{m_e}(\mathbf{v}\times\mathbf{B}) = \mathbf{a}_r(\mathbf{r}) + \mathbf{a}_L. \qquad (2)$$

Here, e and m_e are the electric charge and the mass of electrons, and $\mathbf{E}$ and $\mathbf{B}$ denote the electric and magnetic fields, respectively. $\mathbf{a}_r(\mathbf{r})$ is the radial component of the acceleration due to the electric force, whereas $\mathbf{a}_L$ is the non-radial component due to the Lorentz force. Using the acceleration $\mathbf{a}$ due to the external forces along with the terms responsible for Coulomb collisions and wave-particle interactions of kinetic turbulence, the kinetic transport equation can be described as follows:

$$\frac{\partial f(\mathbf{r},\mathbf{v},t)}{\partial t} + (\mathbf{v}\cdot\nabla_{\mathbf{r}})f(\mathbf{r},\mathbf{v},t) + (\mathbf{a}\cdot\nabla_{\mathbf{v}})f(\mathbf{r},\mathbf{v},t) = \left(\frac{\delta f}{\delta t}\right)_{cc} + \left(\frac{\delta f}{\delta t}\right)_{wp}. \qquad (3)$$

Here, the electron velocity distribution function is expressed in the position ($\mathbf{r}$), velocity ($\mathbf{v}$) and time (t) domains, and $(\delta f/\delta t)_{cc}$ and $(\delta f/\delta t)_{wp}$ include the effects of Coulomb collisions and kinetic turbulence, respectively. In the coordinates of the radial distance r, the velocity v, and the parameter including the pitch angle θ between the velocity and magnetic field vectors ($\mu \equiv \cos\theta$), Equation (3) becomes

$$\frac{\partial f}{\partial t} + v\propto\frac{\partial f}{\partial r} + a_r(r)\left(\propto\frac{\partial f}{\partial v} + \frac{(1-\propto^2)}{v}\frac{\partial f}{\partial\propto}\right) + \frac{v}{r}(1-\mu^2)\frac{\partial f}{\partial\mu} = \left(\frac{\delta f}{\delta t}\right)_{cc} + \left(\frac{\delta f}{\delta t}\right)_{wp}. \qquad (4)$$

The Coulomb collisions with Maxwellian backgrounds of electrons and protons have been employed in the solar wind environments [16]. The term associated with the Coulomb collisions [32] can be expressed as:

$$\left(\frac{\delta f}{\delta t}\right)_{cc} = c_{v,e}\left\{\left[\mathrm{erf}\left(\frac{v}{v_{\mathrm{th},e}}\right) - G\left(\frac{v}{v_{\mathrm{th},e}}\right)\right]\times \frac{1}{2v^3}\frac{\partial}{\partial\propto}\left[(1-\propto^2)\frac{\partial f}{\partial\propto}\right] + \frac{1}{v^2}\frac{\partial}{\partial v}\left[G\left(\frac{v}{v_{\mathrm{th},e}}\right)v\frac{\partial f}{\partial v}\right] + \frac{1}{v^2}\frac{\partial}{\partial v}\left[\frac{2v^2}{v_{\mathrm{th},e}^2}G\left(\frac{v}{v_{\mathrm{th},e}}\right)f\right]\right\} + c_{v,p}\left\{\left[\mathrm{erf}\left(\frac{v}{v_{\mathrm{th},p}}\right) - G\left(\frac{v}{v_{\mathrm{th},p}}\right)\right]\times \frac{1}{2v^3}\frac{\partial}{\partial\propto}\left[(1-\propto^2)\frac{\partial f}{\partial\propto}\right] + \frac{1}{v^2}\frac{\partial}{\partial v}\left[G\left(\frac{v}{v_{\mathrm{th},p}}\right)v\frac{\partial f}{\partial v}\right] + \frac{1}{v^2}\frac{\partial}{\partial v}\left[\frac{2v^2}{v_{\mathrm{th},p}^2}\frac{m_e}{m_p}G\left(\frac{v}{v_{\mathrm{th},e}}\right)f\right]\right\}, \qquad (5)$$

where m_p/m_e is the proton-to-electron mass ratio and $v_{\mathrm{th},e}$ and $v_{\mathrm{th},p}$ are the thermal velocities of the background Maxwellian electrons and protons. $\mathrm{erf}(x)$ and $G(x)$ are the error function and the Chandrasekhar function, respectively. The collision frequencies corresponding to the collisions with the Maxwellian background electrons ($c_{v,e}$) and protons ($c_{v,p}$) are given by:

$$c_{v,e} = \frac{4\pi n_0 e^4 \ln\Lambda}{m_e^2}, \qquad (6)$$

$$c_{v,p} = \frac{4\pi n_0 e^4 \ln\Lambda}{m_p^2}, \qquad (7)$$

where n_0 and $\ln\Lambda$ are the plasma density and the Coulomb logarithm.

To model the terms for wave-particle interaction, we consider the resonant scattering of electrons by right-handed polarized whistler waves as a main wave-particle interaction mechanism in the turbulent plasma system. Considering the cyclotron resonance of electrons with waves propagating parallel to the guiding magnetic field $\mathbf{B}_0$, the resonant particles satisfy the following condition:

$$\omega_r(k) = v\mu k_{\parallel} + n\Omega_e, \qquad (8)$$

where ω_r and k are the oscillatory wave frequency and the wavenumber, respectively, and $\Omega_e = |e|B_0/m_e c$ is the electron gyrofrequency. The integer $n \neq 0$ must be finite for cyclotron resonance through the parallel waves. In the whistler regime ($\omega_r < \Omega_e$), the magnetic power spectrum [18, 22] can be described as follows:

$$P_B(k) = A\,\frac{c}{\Omega_e}\left|\frac{kc}{\Omega_e}\right|^{-s}, \qquad (9)$$

where A is the normalization constant, and the spectral index s is expected not to exceed 2 [22]. The evolution of the electron distribution function due to wave-particle interaction through whistler turbulence [16–19] can be expressed as

$$\left(\frac{\delta f}{\delta t}\right)_{wp} = \frac{\partial}{\partial \mu}\left(D_{\mu\mu}\frac{\partial f}{\partial \mu} + \frac{1}{m_e}D_{\mu v}\frac{\partial f}{\partial v}\right) + \\ + \frac{1}{v^2}\frac{\partial}{\partial v}\left(v^2\left(\frac{1}{m_e}D_{\propto v}\frac{\partial f}{\partial \propto} + \frac{1}{m_e^2}D_{vv}\frac{\partial f}{\partial v}\right)\right). \quad (10)$$

The diffusion tensor for nonrelativistic electrons is expressed as:

$$\bar{D}_{vv} \equiv \frac{D_{vv}}{\Omega_e (m_e c)^2} = \frac{\pi}{3}\frac{A}{a}\left(\frac{\beta|\mu|}{a}\right)^{\frac{s-1}{3}}(1-\mu^2), \quad (11)$$

$$\bar{D}_{\mu v} \equiv \frac{D_{\mu v}}{\Omega_e (m_e c)} = \frac{D_{v\mu}}{\Omega_e (m_e c)} = \\ = -\frac{\pi}{3}\frac{A}{a}\left[\frac{\mu}{|\mu|}\left(\frac{\beta|\mu|}{a}\right)^{\frac{s-2}{3}} + \frac{\mu}{\beta}\left(\frac{\beta|\mu|}{a}\right)^{\frac{s-1}{3}}\right](1-\mu^2), \quad (12)$$

$$\bar{D}_{\mu\mu} \equiv \frac{D_{\mu\mu}}{\Omega_e} = \frac{\pi}{3}\frac{A}{a}\times \\ \times\left[\left(\frac{\beta|\mu|}{a}\right)^{\frac{s-3}{3}} + 2\frac{\mu}{|\mu|}\frac{\mu}{\beta}\left(\frac{\beta|\mu|}{a}\right)^{\frac{s-2}{3}} + \right. \\ \left. + \left(\frac{\mu}{\beta}\right)^2\left(\frac{\beta|\mu|}{a}\right)^{\frac{s-1}{3}}\right](1-\mu^2). \quad (13)$$

Here, we used dimensionless parameters, $\beta = v/c$ and $a = \omega_{pe}^2/\Omega_e^2$ with the plasma frequency $\omega_{pe} = \sqrt{4\pi n_0 e^2/m_e}$. To consider both weakly magnetized plasmas such as interplanetary, interstellar, and intracluster media ($a \gg 1$) and strongly magnetized plasmas near the stellar magnetosphere ($a < 1$), we examine the properties of wave-particle interactions mediated by whistler turbulence over a wide range of parameter a.

In the kinetic model described by Equation (4), the detailed evolution mediated by Coulomb collisions and wave-particle interactions depends on the initial electron distribution. The electron distribution of thermal plasma is typically modeled as Maxwellian, given by:

$$f_{\mathrm{th},e}(v) = \frac{n_0}{\neq^{3/2} v_{\mathrm{th},e}^3}\exp\left[-\left(\frac{v}{v_{\mathrm{th},e}}\right)^2\right]. \quad (14)$$

While the Maxwellian distribution is suitable for describing the medium in the absence of nonlinear processes such as plasma and magnetohydrodynamic (MHD) waves, shocks, and turbulence, it has been demonstrated that plasma processes associated with such phenomena can accelerate particles. This particle energization results in a distribution that deviates from Maxwellian, known as the kappa distribution [33–35]. The electron kappa distribution is defined as:

$$f_{\kappa,e}(v) = \frac{n_0}{\pi^{3/2} v_{\mathrm{th},e}^3}\frac{\Gamma(\kappa+1)}{(\kappa-3/2)^{3/2}\Gamma(\kappa-1/2)}\times \\ \times\left[1+\frac{1}{(\kappa-3/2)}\left(\frac{v}{v_{\mathrm{th},e}}\right)^2\right]^{-(\kappa+1)}, \quad (15)$$

where $\Gamma(x)$ is the Gamma function and the parameter κ determines the slope of the suprathermal distribution. For $v \gg v_{\mathrm{th},e}$, the kappa distribution follows a power-law form,

$$f_{\kappa,e}(v) \propto v^{-2(\kappa+1)}.$$

A smaller value of κ results in a flatter particle distribution, whereas a larger value of κ makes the kappa distribution closer to Maxwellian. In the subsequent section, we explore how the initial slope of the electron distribution function influences electron transport through whistler turbulence, taking into account the dependence on magnetization.

It is noteworthy that the nature of plasma turbulence and wave-particle interaction mediated by such turbulence could be substantially different from the interpretation obtained through linear theory [36, 37]. Specifically, the effects of nonlinear processes on energy dissipation by whistler waves have been examined through PIC simulations [38, 39]. According to the results of these numerical simulations, the significance of nonlinear damping of whistler waves depends on the fluctuation energy of the turbulence and the magnetization of the plasma system [38]. In weakly magnetized plasma, linear damping dominates over nonlinear damping, indicating that the theory developed in the linear regime could be applicable for examining wave-particle interaction through whistler turbulence. In strongly magnetized plasma, when the turbulent

fluctuation (δB) is sufficiently weak (i.e., $\delta B \leq B_0$), linear theory could be applicable. In this regard, the kinetic model in this work could be suitable for weak turbulence systems in space and astrophysical environments. For systems with strong turbulence ($\delta B \geq B_0$), nonlinear processes should be taken into account in the model, which is beyond the scope of this paper.

3. ELECTRON TRANSPORT THROUGH WAVE-PARTICLE INTERACTION AND ITS DEPENDENCE ON THE MAGNETIZATION OF THE PLASMA SYSTEM

Comparison of $\tau_{\mu v} / \tau_{vv}$ (upper panels) and $\tau_{\mu\mu} / \tau_{vv}$ (lower panels) across parameter space. The plots depict variations with respect to electron velocity β ranging from 10^{-3} to 10^{-1}, and magnetization parameter a spanning from 10^{-4} to 10^{4}. Larger values of a indicate weakly magnetized plasmas, whereas smaller values denote strongly magnetized plasma

Firstly, we examine the acceleration timescales through whistler turbulence and their dependence on the magnetic field strength using the three diffusion coefficients. The acceleration timescales can be derived as follows:

$$\frac{\tau_{vv}}{\Omega_e^{-1}} \equiv \frac{\gamma_e^2 m_e^2 v^2}{\Omega_e^{-1} D_{vv}} = \frac{3a}{A\pi}\beta^2 \left(\frac{\beta|\mu|}{a}\right)^{\frac{1-s}{3}} (1-\mu^2)^{-1}, \quad (16)$$

$$\frac{\tau_{\mu v}}{\Omega_e^{-1}} \equiv \left|\frac{\gamma_e m_e v}{\Omega_e^{-1} D_{\mu v}}\right| =$$

$$= \frac{3a}{A\pi}\beta \left|\frac{\mu}{|\mu|}\left(\frac{\beta|\mu|}{a}\right)^{\frac{s-2}{3}} + \frac{\mu}{\beta}\left(\frac{\beta|\mu|}{a}\right)^{\frac{s-1}{3}}\right|^{-1} \times$$

$$\times (1-\propto^2)^{-1}, \quad (17)$$

$$\frac{\tau_{\mu\mu}}{\Omega_e^{-1}} \equiv \left|\frac{1}{\Omega_e^{-1} D_{\mu\mu}}\right| =$$

$$= \frac{3a}{A\pi}\left|\left(\frac{\beta|\mu|}{a}\right)^{\frac{s-3}{3}} + \frac{2\mu}{|\mu|}\frac{\mu}{\beta}\left(\frac{\beta|\mu|}{a}\right)^{\frac{s-2}{3}} + \right.$$

$$\left. + \left(\frac{\mu}{\beta}\right)^2 \left(\frac{\beta|\mu|}{a}\right)^{\frac{s-1}{3}}\right|^{-1} (1-\mu^2)^{-1}, \quad (18)$$

where γ_e is the Lorentz factor, which is approximately 1 for nonrelativistic particles. To assess the relative importance of pitch angle scattering, the following ratios were calculated:

$$\frac{\tau_{\mu v}}{\tau_{vv}} = \left|\frac{\beta\mu}{|\mu|}\left(\frac{\beta|\mu|}{a}\right)^{-\frac{1}{3}} + \mu\right|^{-1}, \quad (19)$$

$$\frac{\tau_{\mu\mu}}{\tau_{vv}} = \left|\beta^2\left(\frac{\beta|\mu|}{a}\right)^{-\frac{2}{3}} + \frac{2\beta\mu^2}{|\mu|}\left(\frac{\beta|\mu|}{a}\right)^{-\frac{1}{3}} + \mu^2\right|^{-1}. \quad (20)$$

In a strongly magnetized plasma ($a \to 0$), the ratios simplify to:

$$\frac{\tau_{\mu v}}{\tau_{vv}} \to |\mu|^{-1}, \frac{\tau_{\mu\mu}}{\tau_{vv}} \to |\mu|^{-2}, \quad (21)$$

indicating that the relative importance of diffusion in pitch angle space is independent of the particle velocity β and magnetic field strength parametrized by a once the particles satisfy the resonant condition. Given that the pitch angle parameter satisfies $|\propto| < 1$, the following relations hold true in strongly magnetized plasmas:

$$\tau_{vv} < \tau_{\mu v} < \tau_{\mu\mu}. \quad (22)$$

In weakly magnetized plasmas ($a \gg 1$), however, the ratios of these characteristic timescales may vary depending on the particle velocity β and magnetic field strength a.

Fig. 1 shows $\tau_{\mu v} / \tau_{vv}$ and $\tau_{\mu\mu} / \tau_{vv}$ as functions of electron velocity β and magnetization a. A few points were noted: (1) In weakly magnetized plasmas ($a \gg 1$), diffusion processes in the pitch angle space become prominent, whereas a saturated behavior is observed for particle acceleration in sufficiently strong magnetic fields ($a \ll 1$). (2) The dependence on magnetic field strength is more pronounced for accelerating electrons with higher β. Particularly, panels (a) and (d) show that $\tau_{\mu v} / \tau_{vv}$ and $\tau_{\mu\mu} / \tau_{vv}$ exhibit similar asymptotic behaviors for small β and large pitch angles $|\mu| > 0.5$, irrespective of A. Conversely, panels (b), (c), (e), and (f) illustrate that the effects of magnetic field strength on pitch angle scattering are more significant for electrons with larger β. (3) In strongly magnetized plasmas ($a < 1$), $\tau_{\mu v}$ and $\tau_{\mu\mu}$ increase as the pitch angle $|\mu|$ decreases, whereas the opposite behavior is observed

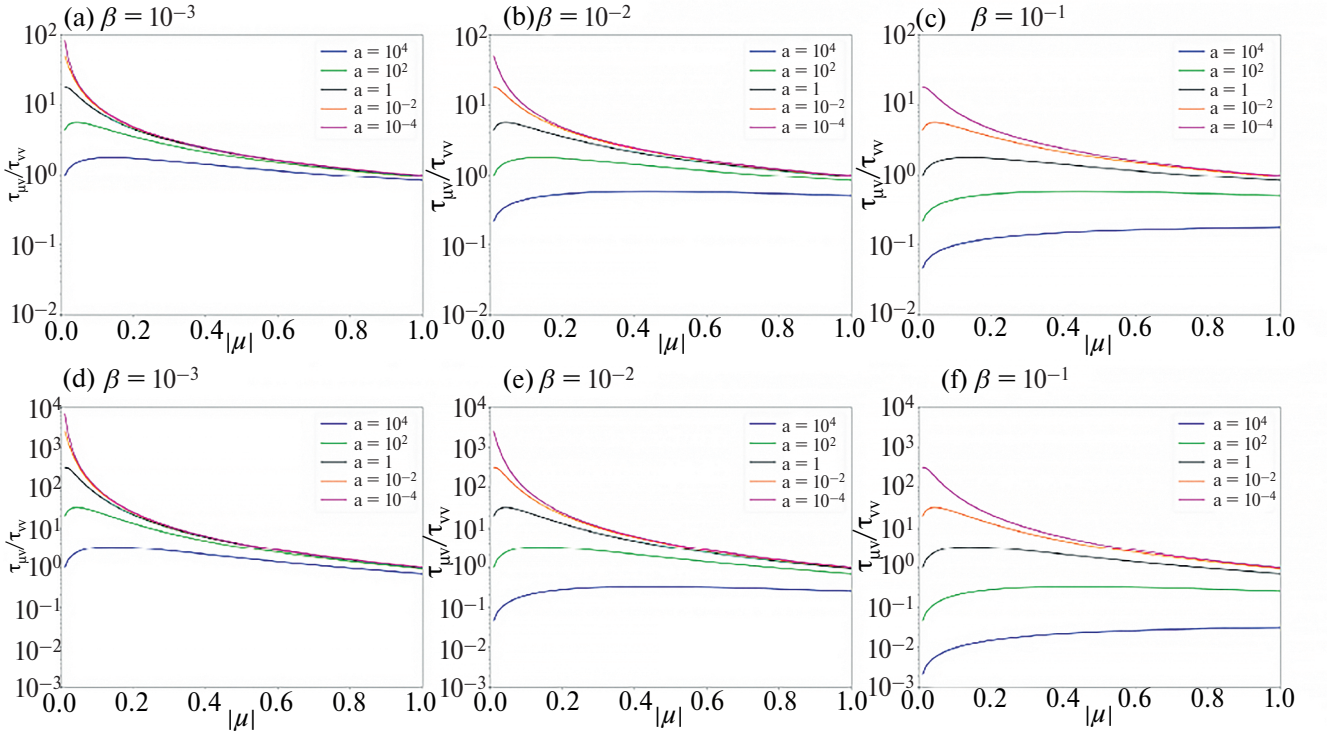

Fig. 1. Comparison of $\tau_{\mu v}/\tau_{vv}$ (upper panels) and $\tau_{\mu\mu}/\tau_{vv}$ (lower panels) across parameter space. The plots depict variations with respect to electron velocity β ranging from 10^{-3} to 10^{-1}, and magnetization parameter a spanning from 10^{-4} to 10^{4}. Larger values of a indicate weakly magnetized plasmas, whereas smaller values denote strongly magnetized plasma

in weakly magnetized plasmas ($a > 1$). This indicates that wave-particle interactions are influenced by the magnetic field strength of the background medium.

Next, we examine the conditions under which the acceleration timescales are dominated by wave-particle interactions over Coulomb collisions. Assuming fixed background temperatures (constant $v_{\mathrm{th},e}$ and $v_{\mathrm{th},p}$), these regimes depend on the magnetic field strength and the initial distribution of suprathermal electrons. Considering the diagonal terms in $\left(\delta f / \delta t\right)_{cc}$ and $\left(\delta f / \delta t\right)_{wp}$ for velocity space diffusion, we have the following expressions:

$$\left(\frac{\delta f}{\delta t}\right)_{cc} \approx c_{v,e}\left\{\frac{1}{v^2}\frac{\partial}{\partial v}\left[G\left(\frac{v}{v_{\mathrm{th},e}}\right)v\frac{\partial f}{\partial v}\right]+\right.$$
$$\left.+\frac{1}{v^2}\frac{\partial}{\partial v}\left[\frac{2v^2}{v_{\mathrm{th},e}^2}G\left(\frac{v}{v_{\mathrm{th},e}}\right)f\right]\right\}+$$
$$+c_{v,p}\left\{\frac{1}{v^2}\frac{\partial}{\partial v}\left[G\left(\frac{v}{v_{\mathrm{th},p}}\right)v\frac{\partial f}{\partial v}\right]+\right.$$
$$\left.=\frac{1}{v^2}\frac{\partial}{\partial v}\left[\frac{2v^2}{v_{\mathrm{th},p}^2}\frac{m_e}{m_p}G\left(\frac{v}{v_{\mathrm{th},e}}\right)f\right]\right\}, \qquad (23)$$

$$\left(\frac{\delta f}{\delta t}\right)_{wp} \approx \frac{1}{v^2}\frac{\partial}{\partial v}\left[v^2\left(\frac{1}{m_e^2}D_{vv}\frac{\partial f}{\partial v}\right)\right]=$$
$$=\frac{1}{v^2}\left[\frac{2v}{m_e^2}D_{vv}\frac{\partial f}{\partial v}+\frac{\partial D_{vv}}{\partial v}\frac{v^2}{m_e^2}\frac{\partial f}{\partial v}+\right.$$
$$\left.+\frac{v^2}{m_e^2}D_{vv}\frac{\partial^2 f}{\partial v^2}\right]. \qquad (24)$$

For $v \gg v_{\mathrm{th},e}$, the Chandrasekhar function can be approximated as $G(v / v_{\mathrm{th},e}) \approx (v / v_{\mathrm{th},e})^{-2} / 2$ and Equation (23) simplifies to:

$$\left(\frac{\delta f}{\delta t}\right)_{cc} \approx c_{v,e}\left\{\frac{1}{v^2}\frac{\partial f}{\partial v}+\right.$$
$$\left.+\frac{1}{2}\left(\frac{v_{\mathrm{th},e}}{v}\right)^2\left[-\frac{1}{v^2}\frac{\partial f}{\partial v}+\frac{1}{v}\frac{\partial^2 f}{\partial v^2}\right]\right\}+$$
$$+c_{v,p}\left\{\frac{1}{v^2}\frac{m_e}{m_p}\frac{\partial f}{\partial v}+\right.$$

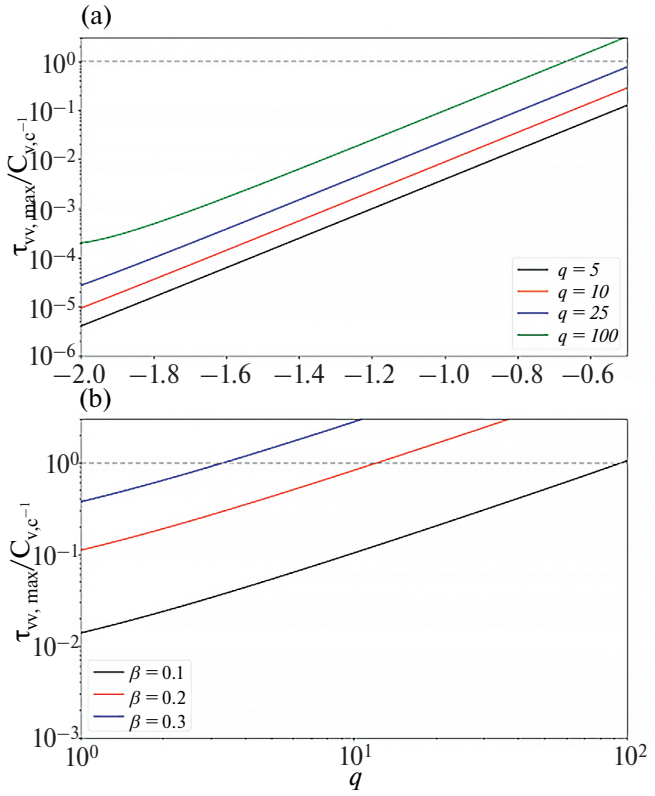

Fig. 2. *a* – Maximum acceleration timescale, $\tau_{\mu v,\max}$, plotted against β for four different q values. **b** – $\tau_{\mu v,\max}$ shown for three different β values across various q values. The electron thermal velocity is set as $v_{\mathrm{th},e}/c = 10^{-3}$. Gray lines indicate $\tau_{\mu v,\max}/c_{v,e}^{-1} = 1$

$$+\frac{1}{2}\left(\frac{v_{\mathrm{th},p}}{v}\right)^2\left[-\frac{1}{v^2}\frac{\partial f}{\partial v}+\frac{1}{v}\frac{\partial^2 f}{\partial v^2}\right]\Bigg\}. \qquad (25)$$

Assuming the suprathermal electrons follow a kappa distribution function, the distribution of high-energy electrons with $v \gg v_{\mathrm{th},e}$ approximates to a power-law tail, $f \propto v^{-q}$. The derivatives of f are expressed as follows:

$$\frac{\partial f}{\partial v} = -qv^{-1}f, \qquad (26)$$

$$\frac{\partial^2 f}{\partial v^2} = q(q+1)v^{-2}f. \qquad (27)$$

Using Equations (26) and (27), Equations (24) and (25) can be rewritten as

$$\left(\frac{\delta f}{\delta t}\right)_{cc} \approx c_{v,e}\left\{-\frac{qf}{v^3}+\frac{1}{2}\left(\frac{v_{\mathrm{th},e}}{v}\right)^2\left[\frac{q(q+2)f}{v^3}\right]\right\}+$$
$$+c_{v,p}\left\{-\frac{m_e}{m_p}\frac{qf}{v^3}+\frac{1}{2}\left(\frac{v_{\mathrm{th},p}}{v}\right)^2\left[\frac{q(q+2)f}{v^3}\right]\right\}, \qquad (28)$$

$$\left(\frac{\delta f}{\delta t}\right)_{wp} \approx \frac{1}{v^2}\left[\frac{q(q-1)D_{vv}}{m_e^2}f - \frac{qvD_{vv}(s-1)\beta^{(s-4)/3}}{3m_e^2 c}f\right]. \qquad (29)$$

Electrons gain energy when

$$\left(\delta f/\delta t\right)_{cc} + \left(\delta f/\delta t\right)_{wp} \geq 0.$$

In this case, we obtain the following inequality for D_{vv}:

$$D_{vv} \geq \left[\frac{q(q-1)}{m_e^2 v^2} - \frac{q(s-1)\beta^{(s-4)/3}}{3m_e^2 vc}\right]^{-1} \times$$
$$\times\left\{c_{v,e}\left[\frac{q}{v^3}-\frac{1}{2}\left(\frac{v_{\mathrm{th},e}}{v}\right)^2\left(\frac{q(q+2)}{v^3}\right)\right]+\right.$$
$$\left.+c_{v,p}\left[\frac{m_e}{m_p}\frac{q}{v^3}-\frac{1}{2}\left(\frac{v_{\mathrm{th},p}}{v}\right)^2\left(\frac{q(q+2)}{v^3}\right)\right]\right\}. \qquad (30)$$

Using the inequality (30), we examine how the slope of the initial distribution of suprathermal electrons could influence the relative importance between Coulomb collisions and wave-particle interactions. For nonrelativistic electrons where $v_{\mathrm{th},e}/c \ll \beta \ll 1$ (or the Lorentz factor $\gamma_e \approx 1$), the acceleration timescale (τ_{vv}) satisfies

$$\tau_{vv} \equiv \frac{\gamma_e^2 m_e^2 \beta^2}{D_{vv}} \leq$$
$$\leq c_{v,e}^{-1}\beta^3(q-1)\left|1-\frac{1}{2}\left(\frac{v_{\mathrm{th},e}}{v}\right)^2(q+2)\right|^{-1}+$$
$$+c_{v,p}^{-1}\beta^3(q-1)\left|\frac{m_e}{m_p}-\frac{1}{2}\left(\frac{v_{\mathrm{th},p}}{v}\right)^2(q+2)\right|^{-1}. \qquad (31)$$

To explore the dependence on the slope of the suprathermal electron distribution, we estimate the maximum acceleration timescales for the two different regimes as follows:

$$\tau_{vv,\max} \approx \begin{cases} 4\beta^3(c_{v,e}^{-1}+\dfrac{m_e}{m_p}c_{v,p}^{-1}), \text{for} q = 5, \\ 2\beta^3\left[c_{v,e}^{-1}\left(\dfrac{v}{v_{\mathrm{th},e}}\right)^2+c_{v,p}^{-1}\left(\dfrac{v}{v_{\mathrm{th},p}}\right)^2\right], \\ \text{for} q \to \infty. \end{cases} \qquad (32)$$

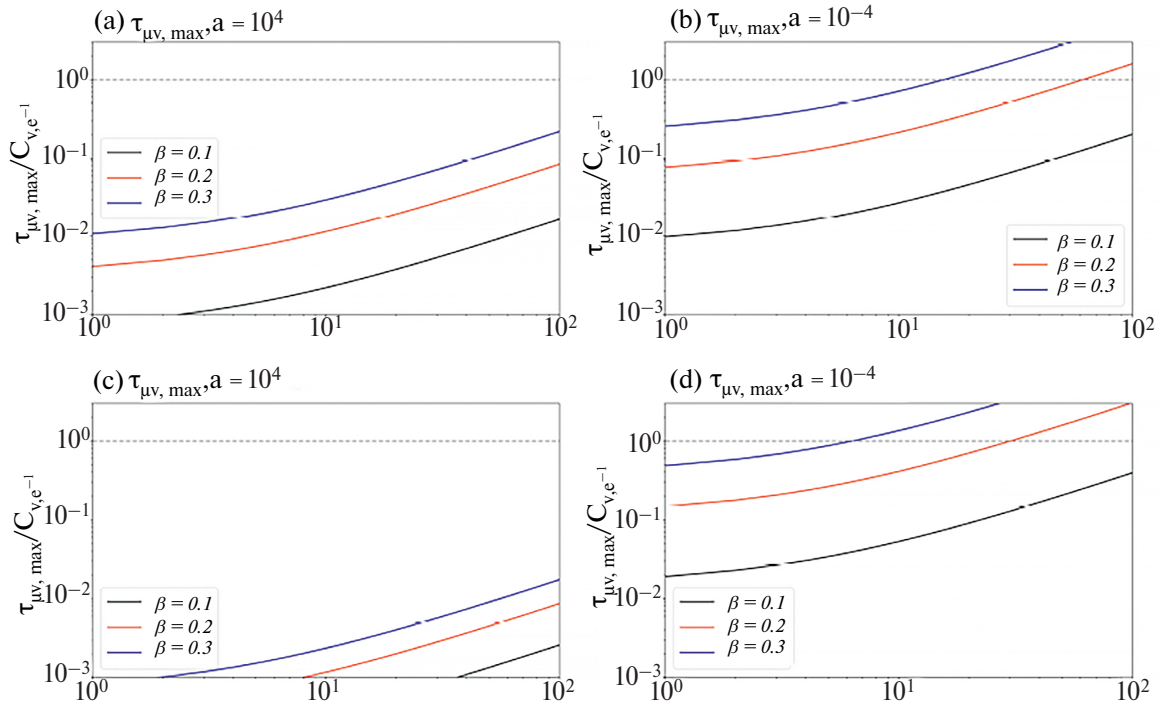

Fig. 3. $\tau_{\mu v,max}$ and $\tau_{\mu\mu,max}$ for weakly (left panels) and strongly (right panels) magnetized plasmas. Here, the electron thermal velocity is assumed as $v_{th,e}/c = 10^{-3}$, and the gray lines display the value $\tau_{max}/c_{v,e}^{-1} = 1$

Because electron velocities satisfy $v/v_{th,e} \gg 1$ and $v/v_{th,p} \gg 1$, the maximum acceleration timescale is much larger when $q \to \infty$. This indicates the evolution of the electron distribution function with a larger q more effectively depends on Coulomb collisions, and such a distribution is likely to resemble a Maxwellian. It is understandable that wave-particle interactions with sufficiently large q are inefficient due to the absence of a sufficient number of resonant particles. Indeed, acceleration timescales become longer regardless of electron velocity for larger q (panel *a* of Fig. 2), and these effects are more pronounced for suprathermal electrons with higher β.

While the analysis in this section has focused on the diagonal terms of the diffusion tensor, it has been demonstrated that the off-diagonal terms, particularly those involving diffusion in pitch angle scattering, are significant in weakly magnetized plasmas. Using equations (19) and (20), we can roughly estimate the maximum values of $\tau_{\mu v}$ and $\tau_{\mu\mu}$ for wave-particle interactions. Applying the inequality (31) to Equations (19) and (20), we obtain

$$\tau_{\mu v} \le \left\{ c_{v,e}^{-1}\beta^3(q-1)\left|1-\frac{1}{2}\left(\frac{v_{th,e}}{v}\right)^2(q+2)\right|^{-1} + \right.$$

$$\left. + c_{v,p}^{-1}\beta^3(q-1)\left|\frac{m_e}{m_p}-\frac{1}{2}\left(\frac{v_{th,p}}{v}\right)^2(q+2)\right|^{-1}\right\} \times$$

$$\times\left|\frac{\beta\mu}{|\mu|}\left(\frac{\beta|\mu|}{a}\right)^{-1/3}+\mu\right|^{-1}, \qquad (33)$$

$$\tau_{\mu\mu} \le \left\{ c_{v,e}^{-1}\beta^3(q-1)\left|1-\frac{1}{2}\left(\frac{v_{th,e}}{v}\right)^2(q+2)\right|^{-1} + \right.$$

$$\left. + c_{v,p}^{-1}\beta^3(q-1)\left|\frac{m_e}{m_p}-\frac{1}{2}\left(\frac{v_{th,p}}{v}\right)^2(q+2)\right|^{-1}\right\} \times$$

$$\times\left|\beta^2\left(\frac{\beta|\mu|}{a}\right)^{-2/3}+\frac{2\beta\mu^2}{|\mu|}\left(\frac{\beta|\mu|}{a}\right)^{-1/3}+\mu^2\right|^{-1}. \qquad (34)$$

Fig. 3 shows the behavior of the two characteristic timescales $\tau_{\mu v}$ and $\tau_{\mu\mu}$ across a wide range of slope parameters q and electron velocities β. In weakly magnetized plasmas ($a = 10^4$), shown in the left panels of Fig. 3, wave-particle interactions

can effectively transport electrons with softer distribution slopes due to enhanced diffusion in pitch angle space. This enhancement occurs even in scenarios where $\tau_{vv} > c_{v,e}^{-1}$, as $\tau_{\mu\mu} < \tau_{\mu v} \ll c_{v,e}^{-1}$ can be satisfied. Conversely, in strongly magnetized plasmas ($a = 10^{-4}$), shown in the right panels of Fig. 3, diffusion in pitch angle space does not significantly enhance efficient transport through wave-particle interactions when collisional effects dominate ($\tau_{vv} > c_{v,e}^{-1}$), as $\tau_{vv} < \tau_{\mu v} < \tau_{\mu\mu}$.

4. CYCLOTRON RESONANCE OF SUPRATHERMAL ELECTRONS AND NATURE OF WHISTLER WAVES

In this section, we derive the conditions for the minimum velocity of resonant electrons and the characteristics of whistler waves corresponding to wave-particle interaction. The criteria described in this section encompass the characteristics of the turbulent power spectrum, such as its power-law slope, and the effects of Coulomb collisions, as depicted in the schematic Fig. (see Fig. 4). Assuming that the energy transferred through whistler turbulence remains constant across spectra with arbitrary slopes, the maximum wavenumber of a flatter spectrum could be larger than that of a steeper spectrum. Additionally, Coulomb collision effects may suppress energy transport to smaller scales, thereby allowing for a larger maximum wavenumber with stronger Coulomb collisional effects. Such wave characteristics could influence particle transport through turbulence by determining the minimum momentum of electrons required for wave-particle interactions.

Considering only the electron collision term, the minimum velocity criterion can be derived using the inequality (31) as follows:

$$\beta \geq \left[\frac{3}{\pi A}(1-\mu^2)^{-1}|\mu|^{(1-s)/3}\left(\frac{v_{\mathrm{th},e}}{c}\right)^3 \times \right.$$

$$\left. \times (q-1)\left(\frac{\Omega_e^{-1}}{\omega_{pe}^{-1}}\right)^{(2s+1)/3}\left(\frac{c_{v,e}^{-1}}{v_{\mathrm{th},e}^{-3}\omega_{pe}^{-1}}\right)^{-1}\right]^{3/(s+2)}. \quad (35)$$

Here, for simplicity, we consider only electron-electron collisions since the collisional timescales satisfy $c_{v,e}^{-1} \ll c_{v,p}^{-1}$. Clearly, more electrons with lower velocities can be energized through wave-particle interactions when collisional timescales are longer. While the minimum velocity increases as the magnetic field strength decreases (or, $|_e^{-1}$ increases), we interpret that these effects could be minor when considering regimes dominated by wave-particle interactions ($|_e^{-1} \ll c_{v,e}^{-1}$). Additionally, a steeper initial slope of the suprathermal electron distribution q leads to a larger minimum velocity, indicating that transport of suprathermal electrons is less likely when q is sufficiently large.

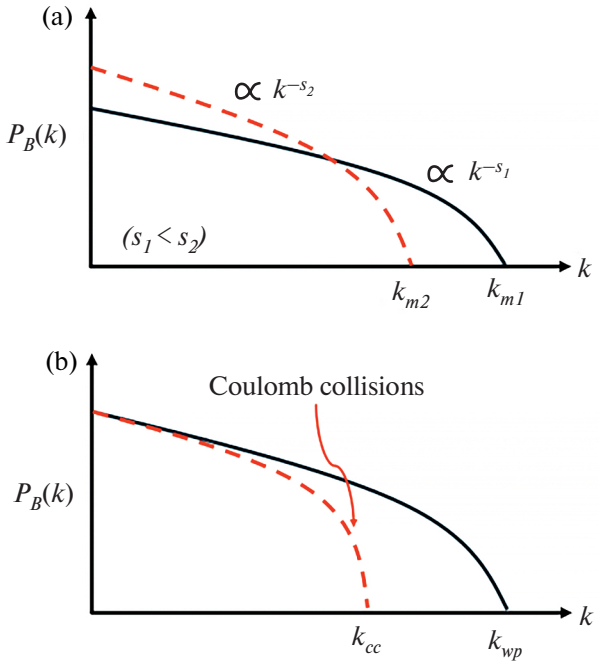

Fig. 4. *a* – Schematic diagrams illustrating whistler turbulence spectra with two different power-law slopes (s_1, s_2). Assuming constant energy transport through whistler turbulence, the maximum wavenumber for a steeper (s_2) spectrum may be smaller than that for a flatter spectrum (s_1) ($k_{m2} < k_{m1}$). *b* – Schematic diagrams demonstrating the influence of Coulomb collisions on turbulent energy transport. Coulomb collisions hinder energy transfer to smaller scales, potentially resulting in a smaller maximum wavenumber (k_{cc}) compared to scenarios without Coulomb collisions (k_{wp})

For low-frequency whistler waves ($\omega_r \ll \Omega_e$), the wavenumber $k_\parallel$ and wavelength $\lambda_\parallel$ for scattering particles are derived as follows:

$$k_\parallel \approx \frac{n\Omega_e}{v\mu}, \quad \lambda_\parallel \equiv \frac{2\pi}{k_\parallel} \approx \frac{2\pi v\mu}{n\Omega_e}. \quad (36)$$

From the inequality (35), we obtain the maximum wavenumber $k_{\parallel,\max}$ and the minimum wavelength $\lambda_{\parallel,\min}$ for wave-particle interactions:

$$\frac{ck_{\parallel,\max}}{\Omega_e} \approx \frac{n}{\mu}\left[\frac{3}{\pi A}(1-\mu^2)^{-1}|\mu|^{(1-s)/3}\left(\frac{v_{\mathrm{th},e}}{c}\right)^3 \times\right.$$

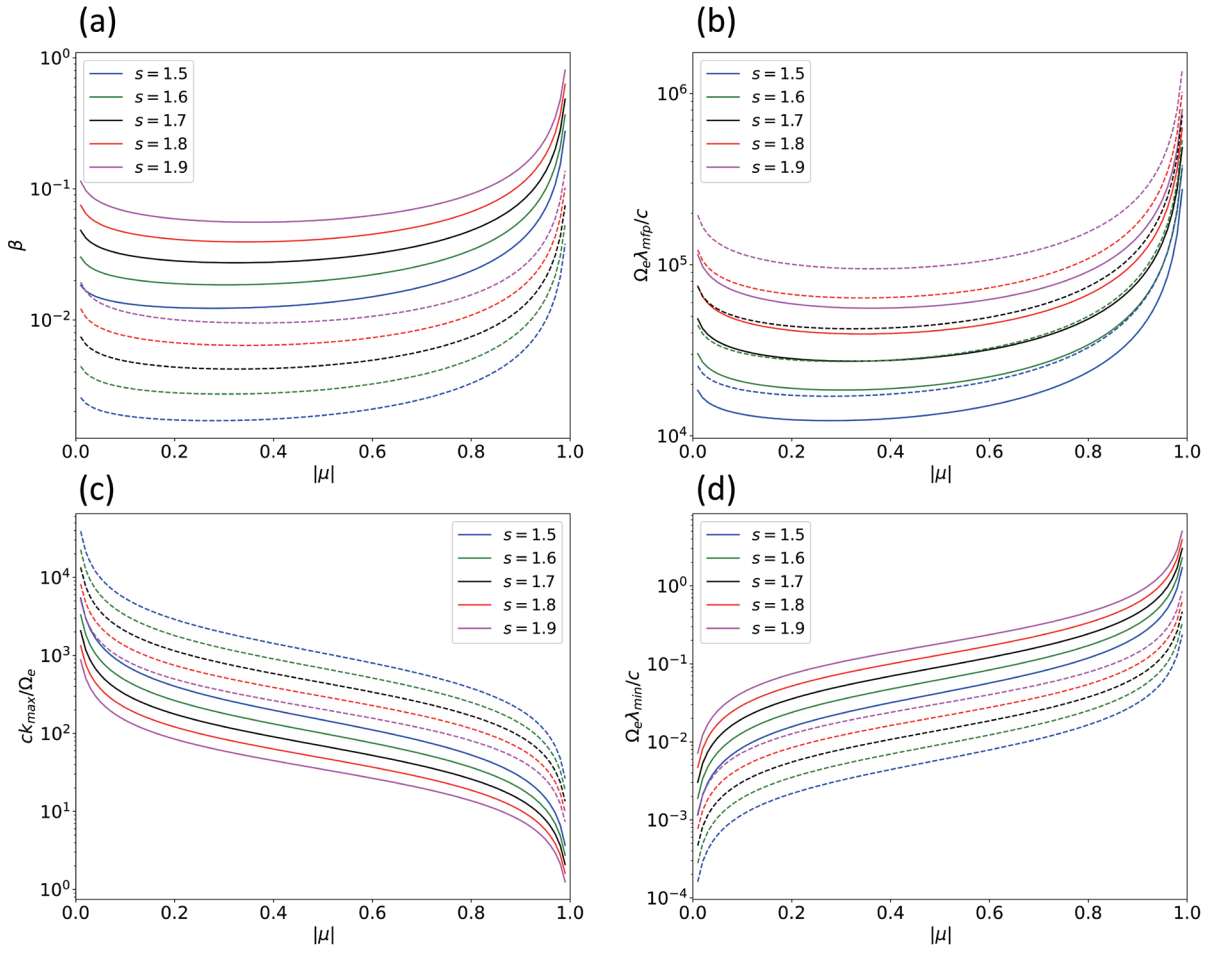

Fig. 5. *a* — Minimum electron velocity, *b* — minimum collisional mean free path, *c* — maximum wavenumber, and *d* — minimum wavelength as functions of pitch angle μ. Solid lines correspond to $c_{v,e}^{-1}/\Omega_e^{-1} = 10^6$, while dashed lines correspond to $c_{v,e}^{-1}/\Omega_e^{-1} = 10^7$. The results are shown for $q = 5$ as an example

$$\times(q-1)\left(\frac{\Omega_e^{-1}}{\omega_{pe}^{-1}}\right)^{(2s+1)/3}\left(\frac{c_{v,e}^{-1}}{v_{\mathrm{th},e}^{-3}\omega_{pe}^{-1}}\right)^{-1}\Bigg]^{-3/(s+2)}, \quad (37)$$

$$\lambda_{\parallel,\min} \approx \frac{2\pi}{k_{\parallel,\max}}. \quad (38)$$

We also consider the minimum collisional length defined as

$$\frac{\Omega_e\lambda_{\mathrm{mfp,min}}}{c} \approx \beta_{\min}\frac{c_{v,e}^{-1}}{\Omega_e^{-1}}. \quad (39)$$

In the criterion (37), the maximum wavenumber decreases as the initial slope of the electron distribution function (q) increases. This indicates that the wavenumber range of wave-particle interactions could be reduced when there are fewer suprathermal electrons (i.e., the spectrum is steeper with larger q).

According to the conditions for resonant scattering and efficient wave-particle interactions, we explore the minimum electron velocity and wave properties relevant to wave-particle interactions across varying power-law slopes of turbulent spectra. The maximum wavenumber $k_{\parallel,\max}$ and minimum wavelength $\lambda_{\parallel,\min}$, derived using the inequality (31) that includes Coulomb collisions and wave-particle interactions, align with the physical insights demonstrated in Fig. 4. Specifically, $k_{\parallel,\max}$ decreases and $\lambda_{\parallel,\min}$ increases as the power-law slope of the turbulent spectra increases. This suggests that turbulence with a flatter spectrum is more efficient at transporting particles. Additionally, as shown by the solid lines in Fig. 5, relatively strong Coulomb collisions can suppress particle transport by reducing $k_{\parallel,\max}$. In contrast, weakly collisional plasmas (represented by dashed lines in Fig. 5) exhibit greater $k_{\parallel,\max}$

values. It is important to note that this analysis generally applies to weakly collisional plasmas where $\lambda_{\parallel,\min} \ll \lambda_{\mathrm{mfp},\min}$.

5. SUMMARY AND DISCUSSION

In this work, we demonstrate how wave-particle interactions through whistler turbulence differ between weakly and strongly magnetized plasmas. In strongly magnetized plasmas (characterized by $a = \omega_{pe}^2 / \Omega_e^2 \ll 1$), the diffusion timescales at large pitch angles ($|\mu| > 0.5$) exhibit saturation for sufficiently small values of a, indicating that strong magnetic fields effectively regulate particle diffusion in pitch angle space. In weakly magnetized plasmas (where $a \gg 1$), on the other hand, large-angle scattering can be enhanced due to the increased magnetization factor a. This enhancement suggests that electron transport via wave-particle interactions may dominate over Coulomb collisions, facilitated by enhanced diffusion in pitch angle space. Additionally, incorporating Coulomb collision effects, we provide conditions for electron transport through whistler turbulence, including the minimum electron velocity and wavelength required for resonant scattering. These findings are broadly applicable to weakly collisional astrophysical plasmas, offering insights into the range of resonant velocities and maximum wavenumbers for wave-particle interactions across a wide range of magnetic field strengths parametrized by a. In such environments, weakly magnetized mediums benefit from efficient transport via wave-particle interactions, particularly when suprathermal particles are present.

We further comment on the significance of investigating particle transport through plasma turbulence in space and astrophysical media. The generation of suprathermal particles is feasible through collisionless shocks or plasma turbulence in various astrophysical environments, with multi-wavelength emissions serving as observational evidence of particle acceleration. While studies on electron transport via whistler turbulence have predominantly focused on non-Maxwellian electron distributions in solar wind environments, similar investigations in diverse astrophysical contexts are warranted. For example, research has shown that velocity anisotropy in interstellar and intracluster media can induce whistler waves [27, 40, 41], potentially maintaining non-Maxwellian electron distributions within localized regions experiencing whistler turbulence. Additionally, it has been shown that suprathermal electrons can be generated by various plasma instabilities in astrophysical media, including whistler, firehose, mirror, and cyclotron instabilities. In particular, current drive exhibited in localized areas, such as the upstream and downstream regions of collisionless shocks, could trigger plasma instabilities that significantly amplify the magnetic field and generate suprathermal particles through waves satisfying cyclotron resonance conditions [26–28, 40–43]. The characteristics of these plasma instabilities and their acceleration efficiency depend on the properties of collisionless shocks, including the shock Mach number, plasma magnetization, and the geometry of the background magnetic field [27, 40]. Moreover, Lower-Hybrid waves could be induced by diamagnetic currents in inhomogeneous plasma systems, which typically propagate in space and astrophysical plasmas, including those with compressible turbulence. The roles of particle acceleration or heating through Lower-Hybrid waves have also been proposed [44, 45]. In this context, it is necessary to conduct further investigations, including the theory of particle transport through various plasma instabilities triggered in astrophysical media, corresponding numerical simulations to support the theory, and complementary observations representing particle acceleration and heating.

REFERENCES

1. *R. Dumont*, Encyclopedia of Nuclear Energy **3**, 479 (2021).
2. *A. A. Schekochihin, S. C. Cowley, and W. Dorland*, Plasma Physics and Controlled Fusion **49**, A195 (2007).
3. *C. Vogt and T. A. Ensslin*, Astronomy and Astrophysics **434**, 67 (2005).
4. *A. H. Minter and S. R. Spangler*, Astrophys. J. **458**, 194 (1996).
5. *R. J. Leamon, C. W. Smith, N. F. Ness, W. H. Matthaeus, and H. K. Wong*, J. Geophys. Res. **103**(A3), 4775 (1998).
6. *S. Regnier*, Astronomy and Astrophysics **581**, A9 (2015).
7. *S. Ni, Y. Chen, C. Li, Z. Zhang, H. Ning, X. Kong, B. Wang, and M. Hosseinpour*, Astrophys. J. Lett. **891**, L25 (2020).
8. *B. Cerutti and G. Giacinti*, Astronomy and Astrophysics **642**, A123 (2020).
9. *C. F. Kennel and F. V. Coroniti*, Astrophys. J. **283**, 694 (1984).

10. *A. A. Schekochihin, S. C. Cowley, W. Dorland, G. W. Hammett, G. G. Howes, E. Quataert, and T. Tatsuno*, Astrophys. J. Supplement Series **182**, 310 (2009).

11. *G. G. Howes*, ArXiv:2402.12829 (2024).

12. *L. Bercic, M. Maksimovic, J. S. Halekas et al.*, Astrophys. J. **921**, 83 (2021).

13. *J. Halekas, P. Whittlesey, D. Larson et al.*, Astrophys. J. Supplement Series 246, 22 (2020).

14. *S. Kim, P. H. Yoon, G. Choe, and L. Wang*, Astrophys. J. **806**, 32 (2015).

15. *P. H. Yoon*, J. Phys.: Conference Series **642**, 012030 (2015).

16. *B. Tang, L. Adhikari, G. P. Zank, and H. Che*, Astrophys. J. **964**, 180 (2024).

17. *B. Tang, G. P. Zank, and V. I. Kolobov*, Astrophys. J. **924**, 113 (2022).

18. *V. Pierrard, M. Lazar, and R. Schlickeiser*, Solar Physics **269**, 421 (2011).

19. *G. P. Zank*, *Transport Processes in Space Physics and Astrophysics*, Springer, Berlin (2014).

20. *O. Allanson, T. Elsden, C. Watt, and T. Neukirch*, Frontiers in Astronomy and Space Sciences **8**, 805699 (2022).

21. *S.-Y. Jeong, D. Verscharen, R. T. Wicks, and A. N. Fazakerley*, Astrophys. J. **902**, 128 (2020).

22. *J. Steinacker and J. A. Miller*, Astrophys. J. **393**, 764 (1992).

23. *C. Vocks, C. Salem, R. P. Lin, and G. Mann*, Astrophys. J. **627**, 540 (2005).

24. *A. Micera, Zhukov A. N., R. Lopez et al.*, Astrophys. J. Lett. **903**, L23 (2020).

25. *A. Micera, Zhukov A. N., R. Lopez et al.*, Astrophys. J. **919**, 42 (2021).

26. *D. Caprioli and A. Spitkovsky*, Astrophys. J. **783**, 91 (2014).

27. *J.-H. Ha, S. Kim, D. Ryu, and H. Kang*, Astrophys. J. **915**, 18 (2021).

28. *A. Bohdan, J. Niemiec, O. Kobzar, and M. Pohl*, Astrophys. J. **847**, 71 (2017).

29. *V. Bresci, M. Lemoine, L. Gremillet, L. Comisso, L. Sironi, and C. Demidem*, Phys. Rev. D1**06**, 023028 (2022).

30. *L. Comisso and L. Sironi*, Astrophys. J. Lett. **936**, L27 (2022).

31. *C. Vega, S. Boldyrev, V. Roytershteyn, and M. Medvedev*, Astrophys. J. Lett. **924**, L19 (2022).

32. *P. Helander and D. J. Sigmar*, *Collisional Transport in Magnetized Plasmas*, Cambridge Univ. Press, Cambridge (2005), Vol. 4.

33. *P. H. Yoon*, Phys. Plasmas **19**, 052301 (2012).

34. *P. H. Yoon, J. Geophys*. Res.: Space Physics **119**, 7074 (2014).

35. *V. Pierrard, M. Lazar, and S. Stverak*, Frontiers in Astronomy and Space Sciences **9**, 892236 (2022).

36. *N. J. Fisch*, Rev. Mod. Phys. **59**, 175 (1987).

37. *S. I. Popel and V. N. Tsytovich*, Contributions to Plasma Physics **31**, 77 (1991).

38. *O. Chang, S. P. Gary, and J. Wang*, Phys. Plasmas **21**, 052305 (2014).

39. *E. Camporeale and G. Zimbardo*, Phys. Plasmas **22**, 092104 (2015).

40. *S. Kim, J.-H. Ha, D. Ryu, and H. Kang*, Astrophys. J. **913**, 35 (2021).

41. *M. A. Riquelme and A. Spitkovsky*, Astrophys. J. **733**, 63 (2012).

42. *A. R. Bell*, Monthly Notices of the Royal Astronomical Society **353**, 550 (2004).

43. *E. Amato and P. Blasi*, Monthly Notices of the Royal Astronomical Society **392**, 1591 (2009).

44. *I. Shinohara and M. Hoshino*, Adv. Space Res. **24**, 43 (1999).

45. *F. Lavorenti, P. Henri, F. Califano, S. Aizawa, and N. Andre*, Astronomy and Astrophysics **652**, A20 (2021).